

The magnetorotational instability across the dead zone of
protoplanetary disks

M. Reyes-Ruiz

Instituto de Astronomía, UNAM, Apdo. Postal 877, Ensenada, B.C. 22800, México.

Received _____; accepted _____

ABSTRACT

We examine the linear stability of a flow threaded by a weak, vertical magnetic field in a disk with a keplerian rotation profile and a vertical stratification of the ionization degree as that predicted for vast portions of protoplanetary disks. A quasi-global analysis is carried out, where the form of the perturbations in the vertical direction is determined. Considering the ohmic magnetic diffusivity of the gas, the conditions leading to the magnetorotational instability are analyzed as a function of the diffusivity at the disk surfaces, its vertical profile and the strength of the unperturbed magnetic field. For typical conditions believed to prevail in protoplanetary disks at radial distances between 0.1 and 10 AU, where the so-called dead zone is proposed to exist, we find that generally the instability is damped. This implies that, if the MRI is considered the only possible source of turbulence in protoplanetary disks, no viscous angular momentum transport occurs at those radii.

Subject headings: accretion, accretion disks – magnetic fields – MHD – planetary systems – solar system: formation

Disks around classical T-Tauri stars, also called protoplanetary disks (or PP disks hereafter), are commonly modeled as viscous accretion disks. Observed evolutionary trends for the global properties of PP disks have been shown to be roughly consistent with those predicted by accretion disk models (Hartmann et al. 1998, Stepinski 1998). However, the acceptance of such models is justifiably not universal and their precise properties are far from established. Nevertheless, partially on account of the existing theoretical framework, accretion disk models constitute the basis of most current models for protoplanetary disks.

In such models, molecular viscosity being drastically insufficient to explain the observed evolutionary timescales for these objects, an anomalous viscosity is invoked to drive the evolution of PP disks. Albeit their precise origin was not readily identified, turbulence and magnetic fields were suggested, and generally accepted, as responsible of the required anomalous “viscous” torques (Lynden-Bell 1969, Shakura & Sunyaev 1973, Eardley & Lightman 1976). In the seminal work of Balbus & Hawley (1991) the instability of perfectly conducting, keplerian flows, threaded by a weak magnetic field, was identified as an unavoidable factor in the dynamics and magnetic field generation process in accretion disks. Since that time, this so-called magnetorotational instability (also called MRI hereafter) has been shown to lead to self-sustained MHD turbulence capable of transporting angular momentum outwards through the disk while mass is driven toward the central object (Hawley, Gammie & Balbus 1995, Brandenburg et al. 1995, Stone et al. 1996).

As long as magnetic diffusive processes are small enough and a weak magnetic field threads a keplerian disk, the MRI arises and leads to self-sustained turbulence capable of driving disk evolution (Jin 1996, Balbus & Hawley 1998). These conditions are generally met in accretion disks around compact objects but apparently not in extended regions of protoplanetary disks (Gammie 1996, D'alessio et al. 1998). Temperatures less than 1000 K outwards of ~ 1 AU predicted by models of PP disks result in a sharp drop of the ionization degree (Stepinski 1992). Since the magnetic ohmic diffusivity is inversely proportional to the ionization degree this implies the importance of diffusive processes beyond such distances (see also Stepinski, Reyes-Ruiz & Vanhala 1993). There, galactic cosmic rays and other external sources become the principal ionizing agents.

An important feature of the ionization due to such extraneous factors is that, since their effect is shielded as they travel into the disk, the ionization fraction is strongly stratified decreasing from the disk surfaces to the midplane (Dolginov & Stepinski 1994).

Under the assumption that the MRI is the only source of self-sustained turbulence and “viscous” torques in accretion disks, Gammie (1996) proposed that mass transfer in PP disks, beyond the inner hot region, takes place in a layered manner. In the layered accretion scenario angular momentum and mass transfer occurs only through active layers near the disk surfaces, where the magnetic diffusivity is low enough for the MRI to develop, while the gas stagnates in the strongly diffusive “dead zone” around the midplane. The evolution of protoplanetary disks via layered accretion has been calculated by Stepinski (1999) finding that it can be dramatically different from that predicted by “standard” models of PP disks, with vertically uniform viscosity, as those presented by Ruden & Lin (1986), Ruden & Pollack (1991) and Reyes-Ruiz & Stepinski (1995) among others.

Given the importance of having reliable, detailed models for the structure and evolution of PP disks as foundation for theories of planet formation, we believe a critical revision of the layered accretion scenario is justified. We begin this work in the present paper by studying the effect of diffusivity stratification on the linear development of the MRI.

We consider the most important implicit assumptions leading to the scenario of layered accretion (Gammie 1996) are the following. First, that the MRI develops in the active regions leading to MHD turbulence, and angular momentum transport, as it does in homogeneous disks, i.e. disks without diffusivity stratification. Secondly, the stagnant condition giving the dead zone its name in the model of Gammie (1996) follows from the assumption that no significant stresses, of Reynolds or Maxwell type, are present in such region. The first assumption is motivated by the results of the local, linear analysis carried out by Jin (1996) who found that although ohmic magnetic diffusivity can quench the MRI, at least for the minimum mass solar nebula model, the ionization degree in the active layers may be sufficient for the instability to develop. However, as discussed by Sano & Miyama (1999) a quasi-global analysis, incorporating the boundary conditions of the

problem in the z direction and the stratification of the magnetic diffusivity, could yield new constraints on the instability criterion. Moreover, at least this level of nonlocality in the analysis of the MRI is required if one is to say anything about the velocity and magnetic field perturbations, and resulting stresses, induced in the dead zone of PP disks.

The aim of this paper is to analyze in detail the emergence of the MRI across the dead zone of protoplanetary disks. We address the main assumptions of the layered accretion scenario outlined above. In contrast to the recent, similar work by Sano & Miyama (1999) we adopt the simplest geometry and perturbation type for which the MRI is known to arise and focus on the specific effects of a magnetic diffusivity profile as that expected in standard, accretion disk models of PP disks. We seek to analyze the stability criterion and z dependence of the perturbations through the active layers and dead zone. The implications of our results on the dynamics of PP disks are discussed for a wide range of disk models.

1. Formulation of the problem

We consider the quasi-global, linear stability of a keplerian flow threaded by a uniform vertical magnetic field in a medium with z -dependent ohmic diffusivity. Our quasi-global study follows in spirit the analysis by Gammie & Balbus (1994) but we include a variable ohmic diffusivity in the magnetic induction equation. This configuration is considered as a model of the middle portions of protoplanetary disks where the dead zone is proposed to exist (Gammie 1996). As a first approximation to this problem, for reasons purely of mathematical simplicity, we consider only the effect of ohmic magnetic diffusion. The influence of other diffusive processes on the MRI, such as ambipolar diffusion, has been studied by Wardle (1997, 1999) in a local approach. Although such processes are probably important in regions of PP disks, their incorporation into a global analysis is left for future contributions.

In our quasi-global analysis the unperturbed system is considered homogeneous in the radial and azimuthal directions in all properties except the angular velocity, which is a function of the radial distance from the central star. We concentrate on the effect of diffusion on the most unstable modes found in the ideal MHD analysis, those corresponding to destabilized Alfvén waves traveling in the z -direction (Balbus & Hawley 1998). To this end we assume an unperturbed weak magnetic field configuration like $\mathbf{B} = B\hat{z}$ where B is a constant. The equilibrium condition for the flow, in the presence of the gravitational force due to the central star, corresponds to circular rotation with velocity $\mathbf{U} = r\Omega\hat{\phi}$, where Ω is equal to $\sqrt{GM_\star}/r^{3/2}$. This is the simplest disk configuration where the instability arises in the ideal MHD analysis (Balbus & Hawley 1998).

Our starting point are the governing continuity equation,

$$\frac{\partial \rho}{\partial t} + \nabla \cdot (\rho \mathbf{U}) = 0, \quad (1)$$

momentum conservation equation,

$$\frac{\partial \mathbf{U}}{\partial t} + (\mathbf{U} \cdot \nabla \mathbf{U}) = -\frac{1}{\rho} \nabla \left(P + \frac{|\mathbf{B}|^2}{8\pi} \right) + \frac{1}{4\pi\rho} (\mathbf{B} \cdot \nabla \mathbf{B}) - \nabla \Phi, \quad (2)$$

where Φ is the gravitational potential from the central star, and magnetic induction equation,

$$\frac{\partial \mathbf{B}}{\partial t} = \nabla \times (\mathbf{U} \times \mathbf{B} - \eta \nabla \times \mathbf{B}), \quad (3)$$

where η is the ohmic magnetic diffusivity, a function of z in general. The system physical properties; velocity, magnetic field, density, ρ , and pressure, P , are perturbed with axisymmetric linear disturbances of the form $g(z)e^{-\gamma t}$, where $g(z)$ represents the z -dependent amplitude of the perturbation on any of the physical properties of the system.

In the approximation for geometrically thin disks and weak magnetic fields, the restrictions mentioned above allow us to reduce the governing equations, (1)-(3), to a system of coupled equations similar to (8)-(14) of Sano & Miyama (1999). An important simplification in our approach is that, in absence of a toroidal component of the background field, B_ϕ , the r and ϕ components of the momentum and magnetic induction equations, containing the Alfvén modes, decouple from the density, pressure and vertical velocity perturbations.

We represent the perturbations of velocity and magnetic field components as u_r , u_ϕ and b_r , b_ϕ respectively. There is no radial dependence of the perturbation since we restrict our analysis to vertically traveling perturbations. Future contributions will deal with a

more general derivation.

To first order, we can write the equations for the amplitudes of perturbed quantities as:

$$-\gamma u_r - 2\Omega u_\phi - \frac{B}{4\pi\rho} Db_r = 0, \quad (4)$$

$$-\gamma u_\phi + \frac{\Omega}{2} u_r - \frac{B}{4\pi\rho} Db_\phi = 0, \quad (5)$$

$$-\gamma b_r - BDu_r - [\eta D^2 + D\eta D]b_r = 0, \quad (6)$$

$$-\gamma b_\phi - BDu_\phi + \frac{3}{2}\Omega b_r - [\eta D^2 + D\eta D]b_\phi = 0, \quad (7)$$

where D represent the operator d/dz . The density, ρ appearing in equations (4)-(7) is the unperturbed value, taken from the condition of hydrostatic equilibrium in the z direction for an isothermal disk,

$$\rho(z) = \rho_o e^{-z^2/H^2}, \quad (8)$$

where ρ_o is the value of the density at the disk midplane and $H = \sqrt{2}C_s/\Omega$ is the isothermal scale height, with C_s the sound speed in the gas.

These system of equations is solved subject to the following boundary conditions:

$$Du_r|_{z=\pm H_t} = Du_\phi|_{z=\pm H_t} = 0, \quad (9)$$

$$b_r|_{z=\pm H_t} = b_\phi|_{z=\pm H_t} = 0, \quad (10)$$

where H_t is the height above the midplane where the boundary conditions are applied. These boundary conditions correspond to a hot, tenuous halo model for the exterior of the disk, in a force-free state with the assumption of vanishing stress as $|z| \rightarrow \infty$. Such model has been previously used in similar quasi-global analysis of the MRI (Gammie & Balbus 1994, Sano & Miyama 1999). The derivation, presented by Gammie & Balbus (1994), is simplified to equations (9) and (10) in our case of perturbations dependent only on z . We will return to discuss the assumed boundary conditions in section 4.

2. Numerical solution

To ease manipulation in numerically computing the growth rates of the instability, γ , we first normalize all variables by dividing by Ω and making the following substitutions:

$$\hat{\gamma} = \gamma/\Omega, \quad (11)$$

$$\hat{b}_i = b_i/B \quad \text{for } i = r, \phi, \quad (12)$$

$$\eta = \eta_o f(z), \quad (13)$$

$$\hat{z} = z/H, \quad (14)$$

$$\hat{u}_i = u_i/C_s \quad \text{for } i = r, \phi, \quad (15)$$

$$\beta = C_s^2/V_A^2 \quad \text{where } V_A^2 = B^2/4\pi\rho, \quad (16)$$

and

$$R_m = H^2\Omega/\eta_o. \quad (17)$$

Our parameter β is that typically used in plasma physics and our R_m is a magnetic Reynolds number based on the velocity C_s over a scale H . Note that this differs slightly from the traditional definition of R_m in terms of the flow velocity appearing in the magnetic

induction equation. Since ρ depends on z in our model, so does β . We write $\beta = \beta_c/h(z)$, where β_c is the value of the parameter at the disk midplane and $h(z) = e^{\hat{z}^2}$ in our assumed isothermal disk structure. The resulting system of equations can be written as

$$-\hat{\gamma}\hat{u}_r - 2\hat{u}_\phi - \frac{1}{\sqrt{2}}\beta_c^{-1}hD\hat{b}_r = 0, \quad (18)$$

$$-\hat{\gamma}\hat{u}_\phi + \frac{1}{2}\hat{u}_r - \frac{1}{\sqrt{2}}\beta_c^{-1}hD\hat{b}_\phi = 0, \quad (19)$$

$$-\hat{\gamma}\hat{b}_r - \frac{1}{\sqrt{2}}D\hat{u}_r - R_m^{-1}[fD^2 + DfD]\hat{b}_r = 0, \quad (20)$$

$$-\hat{\gamma}\hat{b}_\phi - \frac{1}{\sqrt{2}}D\hat{u}_\phi + \frac{3}{2}\hat{b}_r - R_m^{-1}[fD^2 + DfD]\hat{b}_\phi = 0. \quad (21)$$

The convenience of this normalization is making explicit the dependence of the solution to our problem on the parameters β_c and R_m , it will also depend on the form of the diffusivity profile and indirectly on the boundary conditions.

Now we discretize the variables and coefficients on a set of points $\hat{z}[i] \in [-\hat{H}_t, \hat{H}_t]$ using the notation $g[i]$ to denote the value of the variable g at point i . The derivatives D and D^2 of the variables are approximated with 2nd order centered finite differences on an equispaced grid ($\hat{z}[i] = \hat{z}_{\min} + i * \Delta\hat{z}$). With this, the system of 4 differential equations (18)-(21) becomes a system of $4N$ coupled algebraic equations, where N is the number points in the grid. Corresponding to each point there are 4 equations so that the discretized system of difference equations can be recast in matrix form as

$$\mathbf{A} \begin{pmatrix} \hat{u}_r[1] \\ \hat{u}_\phi[1] \\ \hat{b}_r[1] \\ \hat{b}_\phi[1] \\ \vdots \\ \cdot \\ \cdot \\ \hat{u}_r[N] \\ \hat{u}_\phi[N] \\ \hat{b}_r[N] \\ \hat{b}_\phi[N] \end{pmatrix} - \hat{\gamma} \begin{pmatrix} \hat{u}_r[1] \\ \hat{u}_\phi[1] \\ \hat{b}_r[1] \\ \hat{b}_\phi[1] \\ \vdots \\ \cdot \\ \cdot \\ \hat{u}_r[N] \\ \hat{u}_\phi[N] \\ \hat{b}_r[N] \\ \hat{b}_\phi[N] \end{pmatrix} = 0$$

where the growth rate of our perturbations, $\hat{\gamma}$, are seen to be the eigenvalues of the matrix \mathbf{A} made up of the corresponding terms from the discretization of the system of equations (18)-(21).

We calculate eigenvalues numerically transforming the matrix to upper Hessenberg form and using a QR algorithm. The number of points in the grid was varied from 10 to 50 with no significant change (less than 1%) in the value of the maximum growth rate of the instability. Results shown correspond to a discretization over 20 points for \hat{z} .

The boundary conditions are incorporated rewriting the corresponding equations (18)-(21) for the first and last points of our grid, upon discretization of the conditions (9) and (10) with 2nd order forward and backward differences at the bottom and top disk surfaces respectively.

3. Results

With the application to the middle, poorly ionized portions of PP disks in mind, we compute growth rates and eigenmodes (the form of the perturbations) for weak unperturbed magnetic fields ($\beta_c \geq 0.1$) and moderately diffusive disks. We consider the later condition as $1 < R_m \leq 10^3$ since the parameter R_m can be seen as the ratio of the characteristic diffusive timescale over a length H to the dynamical timescale.

3.1. Case of uniform diffusivity

A global analysis for a homogeneous disk with ohmic diffusivity has recently been presented by Sano & Miyama (1999). Here we repeat their calculation following a slightly different approach, and a different computational method, to ease the comparison to the results for a stratified disk.

To consider a homogeneous diffusivity we simply put $Df = 0$ and $f = 1$ in the system (18)-(21). Figure 1 shows the value of the maximum growth rate of the instability, given by the minimum value of $\hat{\gamma}$ with no imaginary part, as a function of the resistivity reflected in R_m , and the unperturbed magnetic field strength, entering through the parameter β_c .

Fitting a line through the nodes of the function depicted in Figure 1 indicates that the MRI arises as long as the following relation holds:

$$\beta_c < R_m^2 \quad (22)$$

with the stated weak field, weak diffusion restrictions,

$$\beta_c > 1 \text{ and } R_m > 1 \quad (23)$$

We can recast condition (22) in terms of the characteristic timescales of the problem: the diffusion timescale, $t_{\text{dif}} = H^2/\eta$ and the Alfvén wave H -crossing time, $t_A = H/V_A$. For a density stratified disk with constant magnetic diffusivity, the MRI will arise at a given radius if:

$$t_A \lesssim t_{\text{dif}} \quad (24)$$

In order for the instability to develop an Alfvén wave, with the velocity at the disk midplane, must have time to cross the disk before the field diffuses over the same length scale. This result, summarized in condition (22), is equivalent to the requirement that the Lundquist number be greater than unity. The Lundquist number is the ratio of the Alfvén velocity to the “velocity” of drift of magnetic field lines through the conductor due to diffusion. These results are consistent with Sano & Miyama (1999).

3.2. Effect of diffusivity stratification

The calculation of growth rates for a stratified disk is now a simple procedure of prescribing a particular analytic profile for $f(z)$ and following the steps described above.

As we have mentioned we expect the diffusivity to increase rapidly from its minimum value at the disk surfaces. The results we present consider a z -dependence of the ohmic diffusivity like:

$$f(\hat{z}) = e^{(\hat{H}_t^2 - \hat{z}^2)} e^{(\text{Erf}(\hat{H}_t) - \text{Erf}(\hat{z}))/l_o} \quad (25)$$

where Erf refers to the well known Error function. The precise form for this profile and particular choices for l_o will be justified in the discussion section. In addition to β_c and

R_m , in a disk with diffusivity stratification two new parameters l_o and H_t , determine the diffusivity profile at a given radius in the disk and the growth rates of the MRI.

Figures 2 and 3 show the maximum growth rate of the MRI in disks with different β_c , as a function of the stratification parameters R_m (a measure of the ohmic magnetic diffusivity at the surface of the disk) and l_o . The range in both parameters is chosen with the application to PP disks in mind, as we discuss in the next section. Figure 2 corresponds to an unperturbed magnetic field strength with $\beta_c = 10^2$, which we call the strong magnetic field case. Figure 3 corresponds to $\beta_c = 10^4$, referred to as the weak magnetic field case. In both cases the surface of the disk is considered to be at $z = H$.

Depending on the strength of the unperturbed magnetic field the effect of the stratification can be determinant for the existence of the instability. Regions of the disk with characteristic diffusive timescales at the surface less than 10 dynamical timescales, will not be unstable for all unperturbed magnetic fields considered, $\beta_c > 10^2$. The instability will also be generally damped if the stratification is strong $l_o^{-1} \gtrsim 10$. In the next section we discuss the application of our results to PP disks.

Stratification can also affect the form of the perturbations for the fastest growing modes. Figure 4 shows the z -dependent amplitude of the three fastest growing unstable modes for a region with moderate stratification ($l_o^{-1} = 1$) and diffusivity near the stabilizing limit ($R_m = 20$). The surface of the disk is placed at $H_t = 2H$ and the unperturbed magnetic field corresponds to $\beta_c = 10^2$. An interesting feature of this result is the “stratification” of the instability, i.e. the excitation of the instability preferentially in the regions away from the disk midplane. The largest amplitudes in the linear regime, both for velocity and magnetic field perturbations, appear at $z \approx H$.

4. Discussion

We have seen that the behavior of the MRI in stratified media depends crucially on the value and form of the diffusivity profile. It also depends on the magnitude of the unperturbed magnetic field originally present in the disk. In this section we argue what are the likely values of these parameters in the context of PP disk models and discuss plausible consequences of our results. However, before doing this we briefly discuss the implications of modifying some of the main assumptions of our analysis.

4.1. Boundary conditions and field geometry

As discussed in section 1 the adopted boundary conditions follow from modeling the exterior medium as a hot tenuous corona, also called a hot halo by Gammie & Balbus (1994). The continuity of the stress tensor resulting from the perturbations across the disk-halo boundary, and the condition that it vanish at infinity lead to restrictions (9) and (10). While this is apparently a natural choice for isolated disks, different sets of boundary conditions could certainly be constructed and, in principle, these could affect the results presented so far.

Gammie & Balbus (1994) propose two other models for the disk exterior: a tenuous atmosphere, actually the continuation of the disk with an isothermal density profile, and the so-called rigid conductor model, introduced to mimic the effect of having a sink of angular momentum outside the disk. In the former, infinite disk case, no new unstable modes are found by Gammie & Balbus (1994) in comparison to the hot halo model. In the second case, when a load is connected to the field lines, a new mode is found which can be unstable even when all other modes are stable. As discussed by Gammie & Balbus (1994) the new unstable global mode arises for strong seed magnetic fields ($\beta_c \sim 1$). Although the

results of Gammie & Balbus (1994) assume ideal MHD for the disk material, we believe similar conclusions will be found in our case since the introduction of resistivity has not resulted in the appearance of new unstable modes (Jin 1996, Sano & Miyama 1999).

In addition to the nature of the interface, the precise location of the disk-halo boundary is also assumed. This is done in our model through the parameter H_t in equation (25), assumed equal to the isothermal scale height in the results of the previous section. Our choice is motivated by the calculations by D'alessio et al. (1999) of the detailed vertical structure of PP disks in which the density drops rapidly by orders of magnitude after $\sim 1\text{-}2$ isothermal scale heights. The termination of the disk at the scale height H is also an appropriate choice if one considers a polytropic rather than isothermal model for the vertical structure. Alternatively one could argue that the transition from the disk to the halo should be located at the point where β equals unity, i.e. where the magnetic field passes from being a weak dynamical agent, with respect to gas pressure, to being the dominant dynamical factor, as is expected in the corona. Such assumption, with our isothermal disk structure, places H_t at approximately 2 and 3 scaleheights for $\beta_c = 10^2$ and 10^4 respectively. Figure 5 shows the regions of stability and instability as a function of R_m and l_o^{-1} for different values of the parameter β_c . In comparison to figures 2 and 3, and to figure 7 to be discussed below, we see that our results are not changed drastically, although the trend to make the disk more unstable as one increases the vertical extent is significant. As one incorporates into the model regions of lower β , which are more unstable, the damping effect of the poorly ionized middle regions is less important.

4.2. The value of β_c

The parameter β_c depends on the strength of the unperturbed magnetic field seeding the instability. In PP disks a weak seed magnetic field can be expected as a remnant of the

disk formation process out of a magnetized molecular cloud.

Measurements of magnetic fields in molecular clouds indicate that the densest regions, where PP disks are being formed, are commonly threaded by ordered fields with magnitudes around $\sim 10^{-2}$ Gauss (Heiles et al. 1993). If we consider this as the seed field for the MRI, our B , for the typical midplane densities $10^{-9} - 10^{-11}$ gm/cm³ and temperatures 10 – 500 K predicted for PP disks around a few AU, this implies that $10^2 \lesssim \beta_c \lesssim 10^5$.

Somewhat stronger fields would serve to seed the instability near the central star, if it has a significant magnetic field. However, at radial distances $\gtrsim 1$ AU where the dead zone is proposed to exist, such field would most likely be weak, with β_c in the range considered.

4.3. Ionization state of PP disks

We now attempt to justify the range of parameters l_o^{-1} and R_m explored in section 3 on the basis of the expected properties of protoplanetary disks.

Traditionally the evolution of the solar nebula, the archetype of PP disks, has been thought of as consisting of 3 stages. In the first stage, infall from the molecular cloud leads to the formation and growth of an hydrostatic disk. In this so-called formation stage, efficient angular momentum transport resulting from self gravity instabilities leads to a fast evolution which, after some $\sim 10^5$ years, renders most of the disk stable to gravitational instabilities. What follows has usually been called the viscous stage as it is believed that the long term evolution of the disk in this phase is mainly governed by anomalous “viscous” torques resulting on the accretion of mass through the disk and onto the central object. Finally, in the dispersal stage the remaining gas and dust from the process of planet formation is somehow removed. Partly because diffusive, viscous processes act on an ever increasing timescale in the disk, it has been suggested that external agents dominate this

final stage of PP disk evolution (see Hollenbach et al. 2000 and references therein).

As mentioned in the introduction, it is in connection to the origin of the anomalous torques, dominant through the $\sim 10^7$ year lifetime of the viscous stage, that the MRI has become such an important part of accretion disk theory. In this paper, our aim is to determine whether the MRI will arise in poorly ionized portions of PP disks (a prerequisite for generating viscous torques) at the beginning and possibly during the viscous stage. Hence, we consider models for viscous stage protoplanetary disks. Over the last 20 years α -disk models have been constructed addressing the influence of different agents on the disk's viscous evolution (see Ruden & Lin 1986, Ruden & Pollack 1991, Sterzik & Morfill 1994, and Reyes-Ruiz & Stepinski 1995, among others). Apart from temporal and detailed differences in the structure of the disk, the overall properties of the disk generally agree well with the models of the Ruden & Lin (1986). In fact with the exception of the outermost regions, near the outer boundary of the disk, steady state models as those described in detail in Stepinski et al. (1993) reproduce satisfactorily the properties of PP disks at a given instant.

In this paper we adopt such steady state models of PP disks (Stepinski et al. 1993) to describe the radial variation of physical properties as the disks emerge from the formation stage of their evolution. The models incorporate the Shakura & Sunyaev (1973) viscosity prescription and temperature dependent opacity laws as proposed by Ruden & Pollack (1991). The physical properties of the disk are given by a sequence of power laws, described in Stepinski et al. (1993), distributed radially depending on the two basic parameters of the model: the turbulence viscosity parameter of Shakura & Sunyaev, α_{ss} , and the uniform mass accretion rate through the disk, \dot{M} . Values of α_{ss} between 10^{-2} and 10^{-3} are usually quoted from simulations of the MRI in shearing boxes with keplerian differential rotation. As such values seem to be also consistent with observations of T-Tauri disks (D'alessio et al.

1998) we will present results for the limiting values. Again both in models and observations (see review by Calvet et al. 2000) the mass accretion rate ranges from $\sim 10^{-6} M_{\odot}/\text{yr}$, at the beginning of the viscous stage, to $\sim 10^{-8} M_{\odot}/\text{yr}$ through most of their lifetime.

A particular choice of model parameters determines the profiles of midplane density and temperature, surface density, scale height, etc. These, and our isothermal vertical structure model, can be used to calculate the ionization degree throughout the disks following Stepinski et al. (1993). In the innermost disk regions, inwards of ~ 1 AU, we consider thermal ionization of Potassium assumed present in PP disks with solar abundance. As found by Stepinski (1992) in regions with temperature above $\sim 10^3$ K, the ionization degree is high enough to render the disk unstable to the MRI ($R_m \gg 1$). The development of the MRI in this region, called the inner active region (IAR) by Stepinski (1999) proceeds as analyzed by Gammie & Balbus (1994) and is not addressed in this paper.

We concentrate on the regions outwards of the IAR, defined by $r > R_{IAR}$, where R_{IAR} is defined as the radius where the temperature drops below 1000 K. There, ionization is mainly due to the action of galactic cosmic rays penetrating through the disk surfaces. We obtain an upper limit to the ionization fraction neglecting the recombination of electrons onto dust grains and considering only ion reactions as a sink of electrons. Using the ionization and recombinations rates of Stepinski (1992), the ionization fraction, x , can be obtained from the condition of ionization equilibrium,

$$x = 4 \times 10^{-18} \rho(z)^{-1/2} e^{\frac{-S(z)}{2S_o}}, \quad (26)$$

where S_o is the characteristic cosmic ray attenuation density, $\sim 100 \text{ gm/cm}^2$, and $S(z)$ is the integrated surface density from the disk surface to the height z :

$$S(z) = \int_z^{H_t} \rho_c e^{-\frac{z^2}{H^2}} dz. \quad (27)$$

Considering the rapid decrease of the argument, for mathematical simplicity we approximate this function as:

$$S(\hat{z}) \approx \frac{\sqrt{\pi}}{2} \rho_c H (1 - \text{Erf}(\hat{z})), \quad (28)$$

so that the ionization degree can be written as:

$$x(\hat{z}) = 4 \times 10^{-18} \rho_c^{-1/2} h^{-1/2} e^{-(1 - \text{Erf}(\hat{z}))/l_o}, \quad (29)$$

where $l_o^{-1} = \sqrt{\pi} \rho_c H / 4 S_o$. With ohmic diffusivity given by $\eta = 7 \times 10^3 / x$ (Stepinski 1992) we arrive at equation (25) for the diffusivity profile.

In figure 6 we show the radial profiles of the parameters R_m and l_o^{-1} characterizing the diffusivity profile, for a series of specific models of PP disks. Two values of the turbulent viscosity parameter are considered, $\alpha = 10^{-2}$ and 10^{-3} . The mass accretion rate through the disk takes the values 10^{-6} , 10^{-7} and $10^{-8} M_\odot/\text{yr}$. Models with lower α and higher accretion rate are characterized by a higher temperature and surface density at a given radius. For such models the IAR extends farther out in the disk in comparison to corresponding models with higher α and lower \dot{M} . Also, in comparison beyond R_{IAR} their diffusivity is higher, i.e. smaller R_m , as is their stratification reflected in the parameter l_o .

We summarize the results of this section in Figure 7 where a direct comparison of the properties of PP disk models and the regions of stability for different values of β_c is shown. Depending on the value of β_c , marked radii allow us to determine in what regions of the disk the MRI will arise. For example, for the disk model with $\alpha = 10^{-2}$ and $\dot{M} = 10^{-8} M_\odot/\text{yr}$

(short dashed line), even if the seed field is as strong as $\beta_c = 10^2$, in a broad region between several AU and the R_{IAR} (square), located at less than 0.3 AU from Figure 6, the MRI will not arise. For the same model, if $\beta_c = 10^4$, outwards of R_{IAR} the whole disk will be stable. A similar analysis can be performed for the reader’s preferred specific model.

Finally, it is worth stressing that the calculated diffusivities represent a lower bound as we neglect recombination onto dust grains, which can be dominant if their size distribution is similar to that of the ISM (see Reyes-Ruiz & Stepinski 1995).

5. Summary and Conclusions

We have conducted a quasi-global analysis of the behavior of the MRI in the linear regime considering the effects of diffusivity stratification as that expected in protoplanetary disks. As our main result we find that stratification can add to the stabilizing effect of ohmic diffusion found in previous calculations.

Ohmic diffusivity alone, without stratification, will damp the MRI if $R_m \lesssim 10$, regardless of the strength of the unperturbed magnetic field. Weak seed magnetic fields, $\beta_c \gtrsim 10^4$, will become stable if $R_m \lesssim 100$, i.e. if the diffusion timescale is up to 100 times longer than the dynamical timescale. In addition, the stabilizing effect of stratification is significant when it is characterized by values of the parameter $l_o^{-1} \gtrsim 1$, i.e. when the surface density is greater than $S_o \approx 100 \text{ gm/cm}^2$.

5.1. Revised model of PP disks

If the MRI is the only source of turbulence and anomalous viscosity in protoplanetary disks, our results suggest the necessity of a revision of standards models. The calculation

of properties of these revised models, time dependent in essence, is out of the scope of this paper. However, one can speculate on a plausible structure of the revised PP disk models based on the dynamical agents operating at different radii.

In most of the models, outwards of R_{LAR} there is a broad region where the MRI does not operate. The flow in such region would not be turbulent and, in absence of anomalous viscous torques, mass would accumulate in a stable “dead” region (DR).

In some models, for example the one with $\alpha = 10^{-2}$ and $\dot{M} = 10^{-7} M_{\odot}/\text{yr}$, the instability can be excited also in the outermost parts of the disk. This could occur first in a “stratified” manner (as shown in figure 4) due to the strong stratification of the diffusivity. Whether such excitation leads, in the nonlinear regime, to a layered accretion scenario as proposed by Gammie (1996), is the subject of numerical simulations. We propose the existence of a region of layered accretion (LAR) with the cautionary comment that, according to our linear analysis, significant velocity and magnetic field perturbations will also be present in the middle “dead” zone. These could possibly lead, in the nonlinear regime, to somewhat smaller, but non-zero viscous torques in the so-called dead zone.

Regions at a still greater distance from the central object are less diffusive and less stratified, so the operation of the MRI in such regions would be again similar to that in homogeneous disk and turbulence can be generated across the whole vertical extent of the disk in what we call the outer active region (OAR). In conclusion, the results derived in this paper with the assumptions discussed above lead to a revised model for the structure of protoplanetary disks as schematically illustrated in figure 8.

5.2. Caveats of our analysis

We end this contribution pointing out potentially important inconsistencies in our analysis which could affect our conclusions.

First, it is clear that our disk models are dynamically inconsistent. They are derived assuming a constant turbulent viscosity parameter α which, as we show in this paper, is not justified if turbulence is due to the MRI. At most, we could argue that such models reflect the properties of PP disks as they emerge from the self-gravitating formation stage to the viscous evolutionary phase where the MRI is believed to be the dominant player in the transport of angular momentum. Our assumption is made as a means to show the necessity of revising the standard, constant α models of protoplanetary disks as well as the layered accretion scenario.

A similar inconsistency is also present in the calculation of the vertical diffusivity profile since, as shown by Dolginov & Stepinski (1994), if the turbulence in the disk involves a tangled magnetic field, the shielding of cosmic rays can be significantly larger than estimated here. This effect will certainly be important in the nonlinear regime of the instability.

Acknowledgements The author is thankful to Adriana Gazol for helpful comments at the beginning of this work. This work has been supported by CONACYT project J22990E.

REFERENCES

Balbus, S.A. & Hawley, J.F. 1991, *ApJ*, 376, 214

Balbus, S.A. & Hawley, J.F. 1998, *Rev. Modern Physics*, 70, 1

Brandenburg, A. et al. 1995, *ApJ*, 446, 741

Calvet, N., Hartmann, L. & Strom, S. 2000, in Mannings, V., Boss, A.P., Russell, S.S., eds, *Protostars and Planets IV*, University of Arizona Press: Tucson.

D'alessio, P., Canto, J., Calvet, N. & Lizano, S., 1998, *ApJ*, 500, 411

D'alessio, P., Calvet, N., Hartmann, L., Lizano, S. & Canto, J., 1999, *ApJ*, 527, 893

Dolginov, A. & Stepinski, T.F. 1994, *ApJ*, 427, 377

Eardley, D.M. & Lightman, A.P. 1976, *ApJ*, 200, 181

Gammie, C.F. 1996, *ApJ*, 457, 355

Hartmann, L., Calvet, N., Gullbring, E. & D'alessio, P. 1998, *ApJ*, 495, 385

Hawley, J.F., Gammie, C.F. & Balbus S.A. 1995, *ApJ*, 440, 742

Hawley, J.F., Gammie, C.F. & Balbus S.A. 1996, *ApJ*, 464, 690

Heiles, C. et al 1993, in Levy, E.H. & Lunine, J.I., eds, *Protostars and Planets III*. University of Arizona Press, Tucson, p279

Hollenbach, D.J., Yorke, H.W. & Johnstone, D. 2000, in Mannings, V., Boss, A.P., Russell, S.S., eds, *Protostars and Planets IV*, University of Arizona Press: Tucson.

Jin, L. 1996, *ApJ*, 457, 798

Lynden-Bell, D. 1969, *Nature*, 223, 690

Reyes-Ruiz, M. & Stepinski, T.F. 1995, *ApJ*, 438, 750

Ruden, S.P. & Pollack, J.B. 1991, *ApJ*, 375, 740

Ruden, S.P. & Lin, D.N.C. 1986, *ApJ*, 308, 883

Sano, T. & Miyama, S.M. 1999, *ApJ*, 515, 776

Shakura, N.I., & Sunyaev, R.A. 1973, *A&A*, 24, 337

Stepinski, T.F. 1992, *Icarus*, 97, 130

Stepinski, T.F. 1998, *ApJ*, 507, 361

Stepinski, T.F. 1999, in Proceedings of the 30th Annual Lunar and Planetary Science Conference, abstract no.1205

Stepinski, T.F., Reyes-Ruiz, M. & Vanhala, H.A.T. 1993, *Icarus*, 106, 71

Stone, J.M., Hawley, J.F. & Gammie C.F., Balbus S.A. 1996, *ApJ*, 463, 656

Umebayashi, T. & Nakano, T. 1988, *Prog. Theor. Phys. Suppl.*, 96, 151

Wardle, M. 1997, in Wickramasinghe D., Ferrario L., Bicknell G., eds, Proc. IAU Colloq. 163, Accretion Phenomena and Related Outflows. ASP Press: San Francisco, p.561

Wardle, M. 1999, *MNRAS*, 307, 849

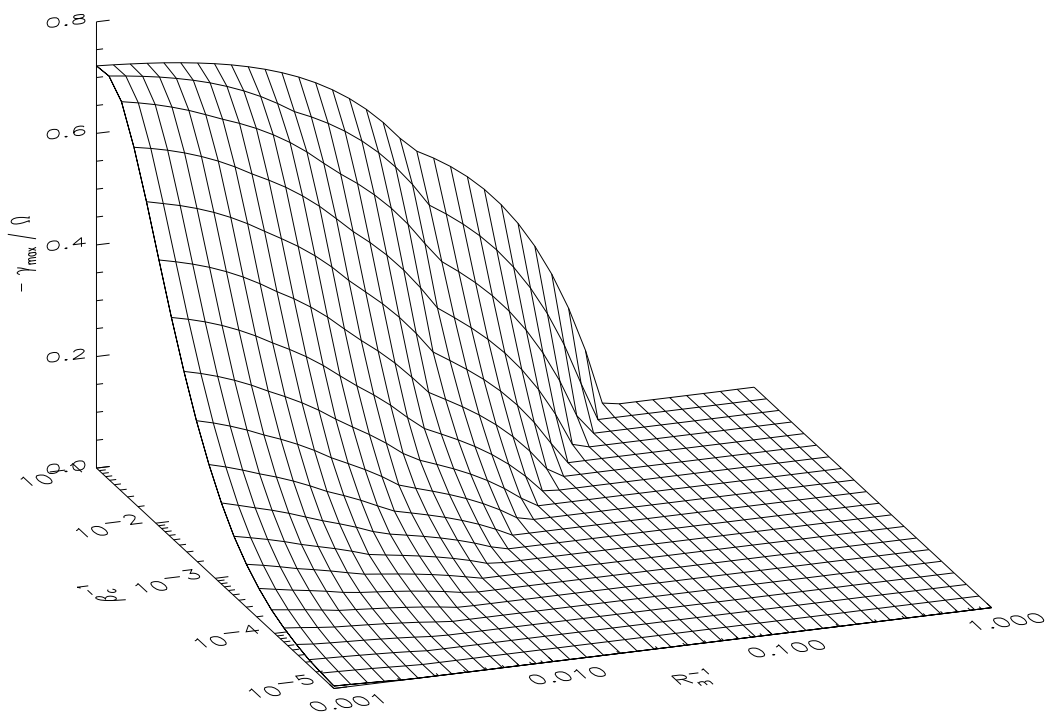


Fig. 1.— Maximum growth rate of the magnetorotational instability as a function of β_c and R_m , in a medium with uniform ohmic diffusivity.

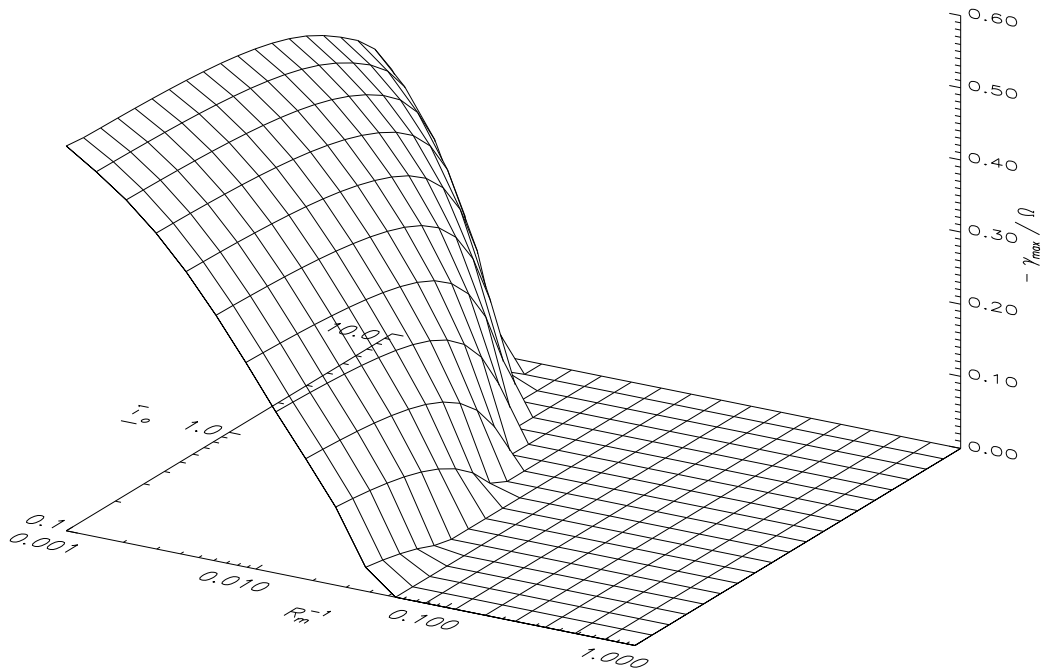


Fig. 2.— Maximum growth rate of the MRI in a stratified disk with $\beta_c = 10^2$ as a function of l_o^{-1} and R_m . The diffusivity profile is given by equation (25) with the surface of the disk placed at $z = H$.

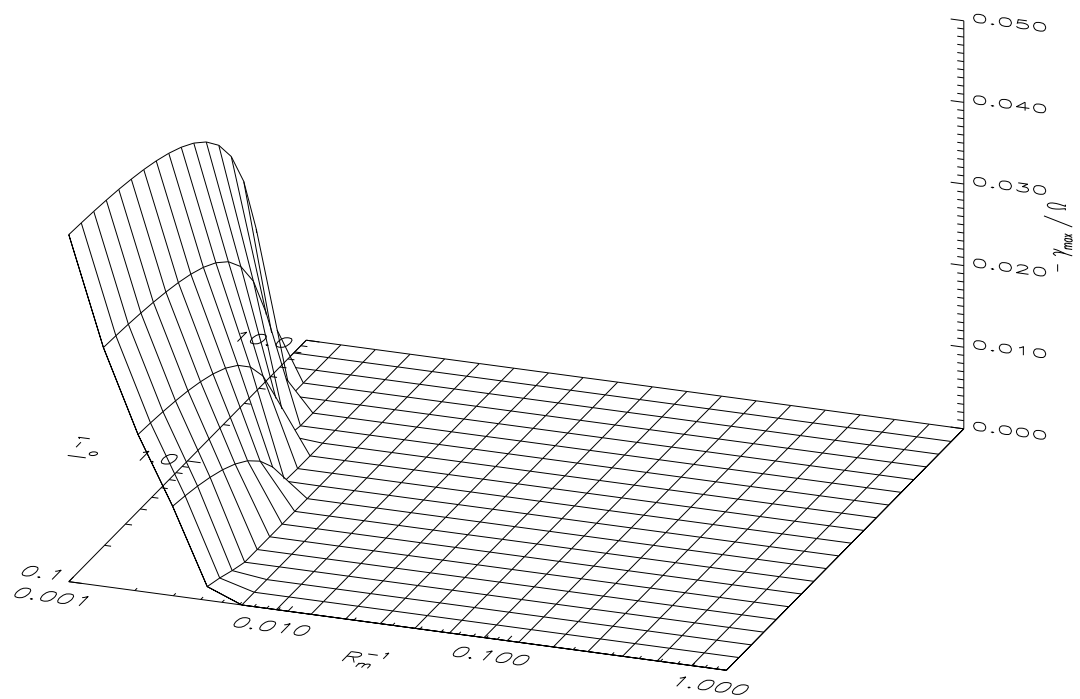


Fig. 3.— Same as figure 2 but for an unperturbed magnetic field corresponding to $\beta_c = 10^4$.

Notice the change of scale in the z axis.

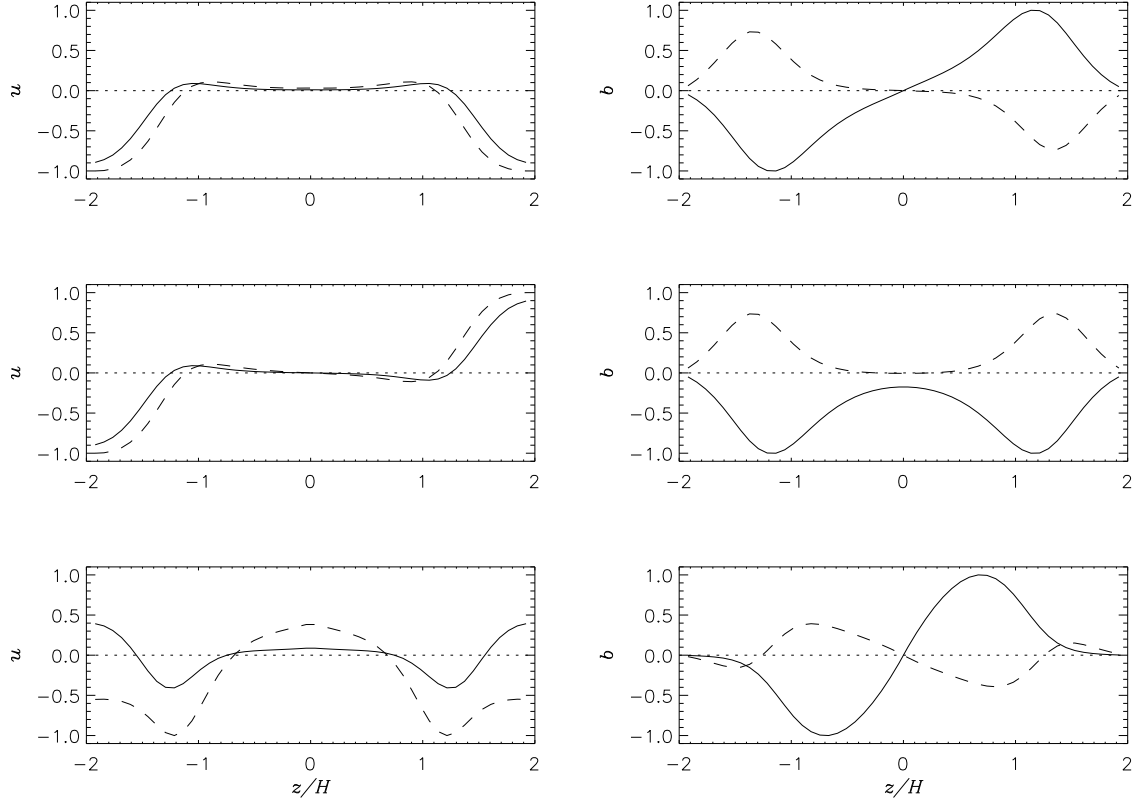


Fig. 4.— Fastest growing modes (from top to bottom) of the MRI in a stratified disk with $R_m = 20$, $l_o^{-1} = 1$ and $H_t = 2H$. The unperturbed magnetic field corresponds to $\beta_c = 10^2$. Left and right panels correspond to velocity and magnetic field perturbations respectively. In all cases the solid (dashed) line indicates the azimuthal (radial) component.

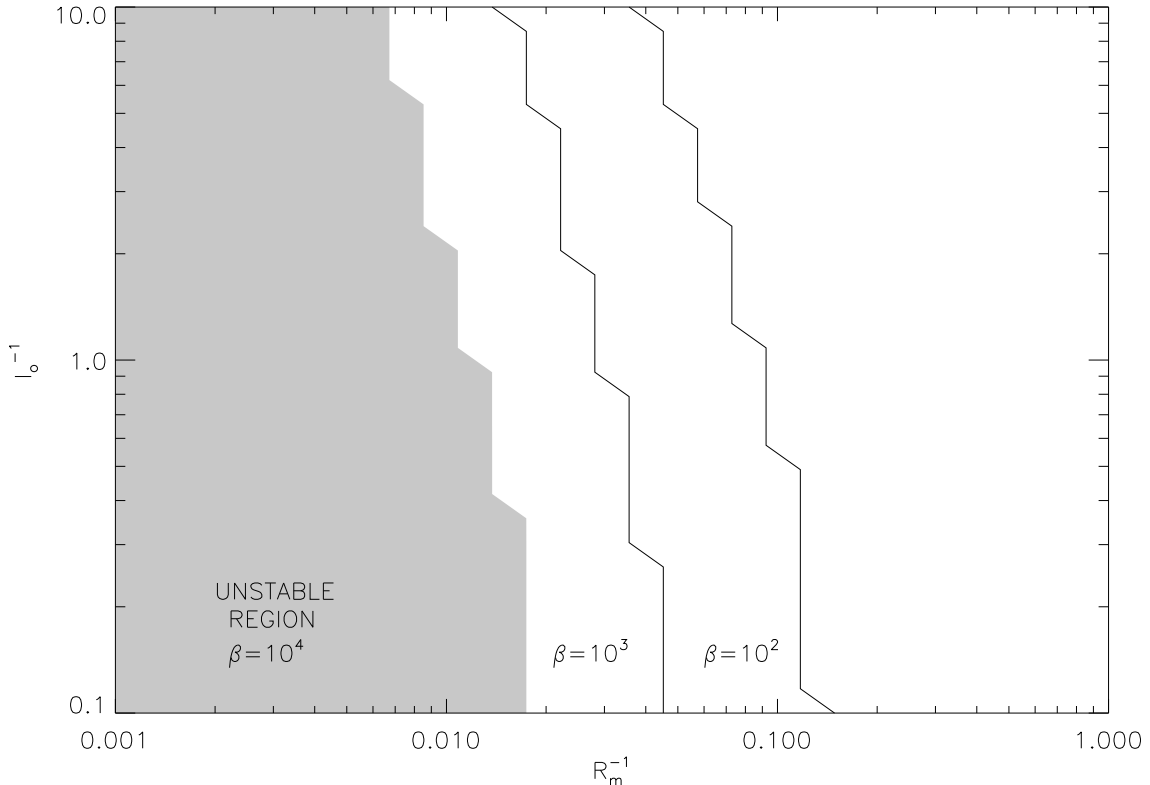


Fig. 5.— Regions of $l_o^{-1} - R_m^{-1}$ parameter space where the MRI arises for $H_t = 3H$. The shaded region illustrates unstable combinations of the diffusivity parameters for $\beta_c = 10^4$. The 2 thin solid lines indicate the boundary of stability in disks with $\beta_c = 10^3$ (lower line) and $\beta_c = 10^2$ (upper line).

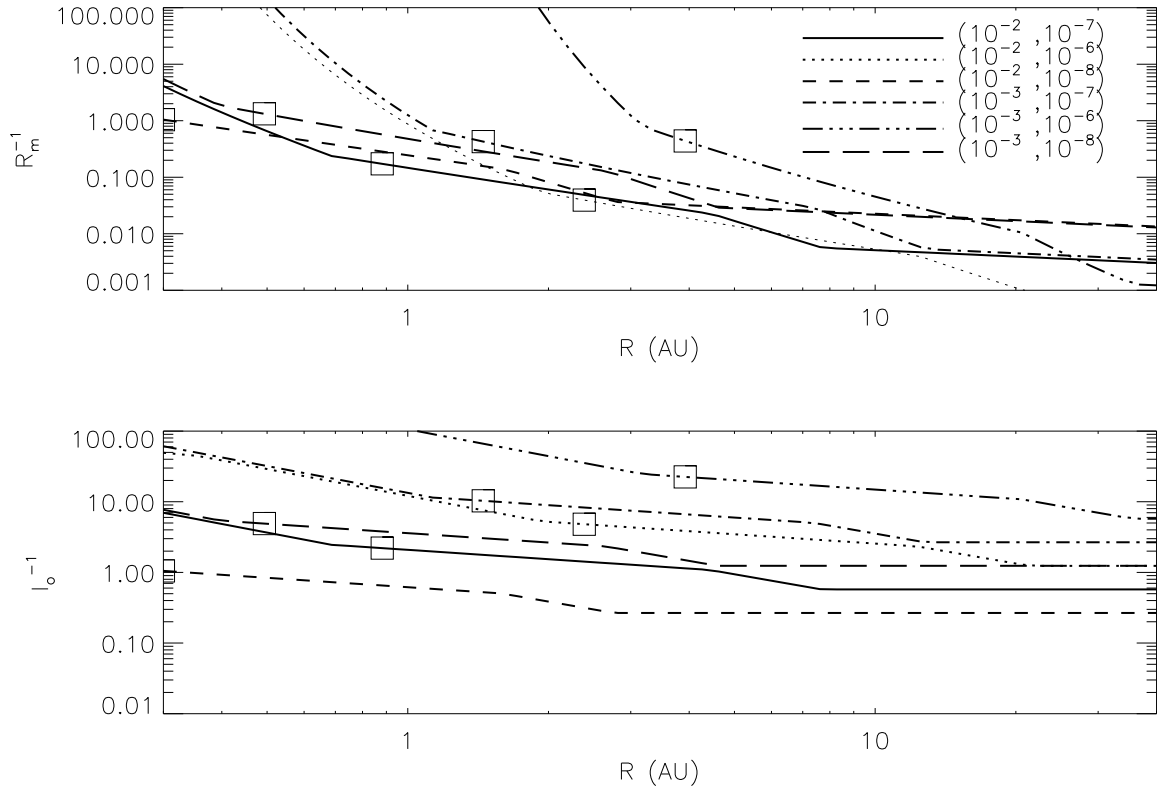


Fig. 6.— Radial profiles of ionization properties, reflected in the parameters R_m and l_o^{-1} for different models of protoplanetary disks. In the legend of linestyles the first number indicates the value the α parameter and the second the mass accretion rate in solar masses per year. For each model the square indicates the position of the R_{IAR} .

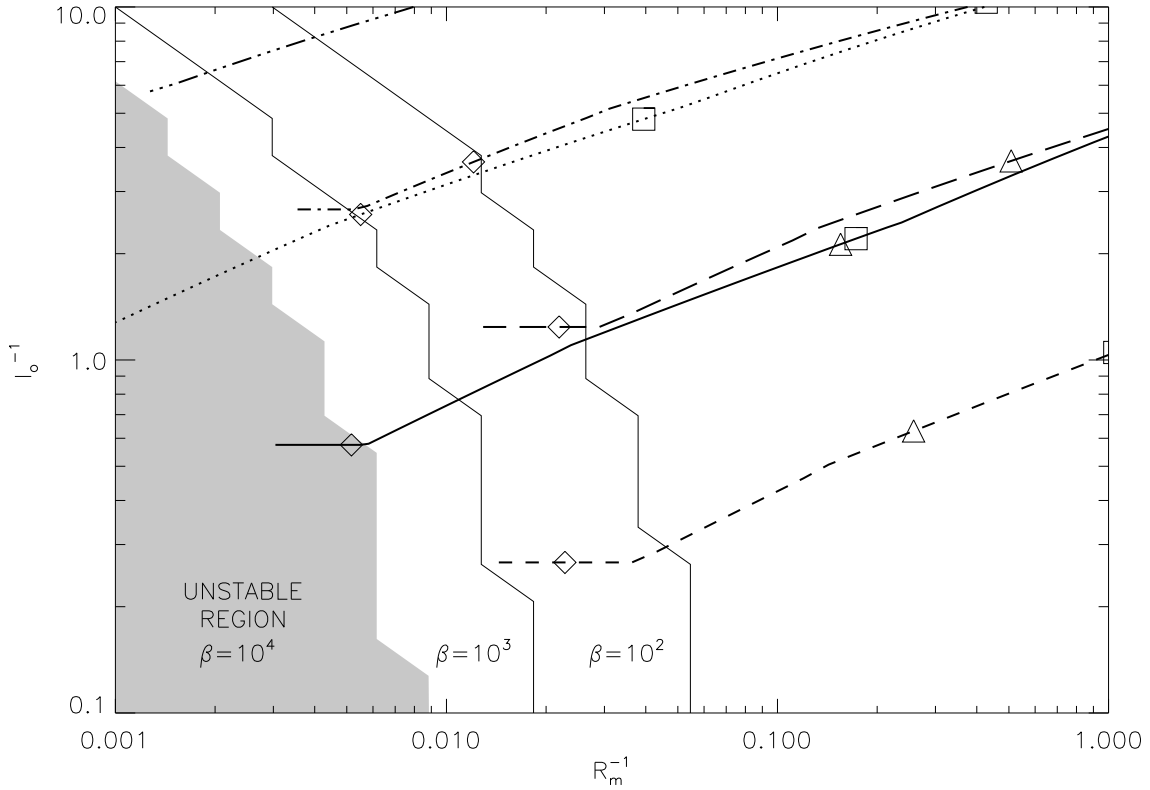


Fig. 7.— Comparison of R_m and l_o^{-1} values for various PP disk models with the stability conditions resulting from our analysis. Disk models and corresponding linestyles are the same as those presented in figure 5. The leftmost edge of such lines correspond to the value of R_m^{-1} and l_o^{-1} at 60 AU. Over each line the square marks the R_{IAR} and the triangle and diamond mark where $R = 1$ and $R = 10$ AU respectively.

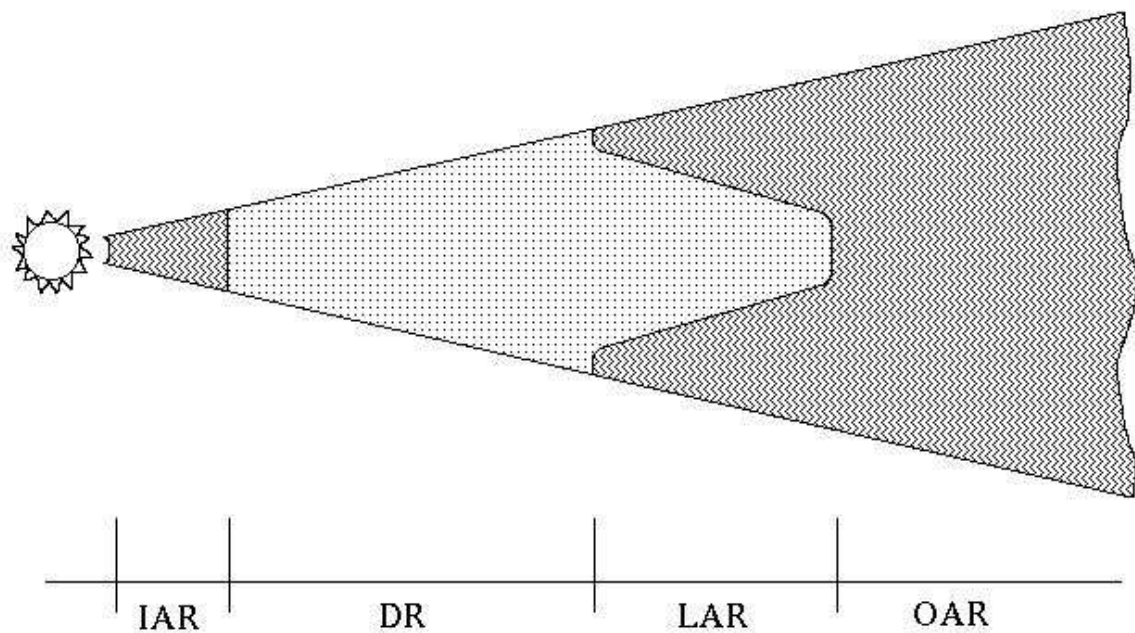


Fig. 8.— Illustration of the general structure of PP disks, indicating active and dead regions as suggested by our results.